Volume 10 | Number 33 | 7 September 2014 | Pages 6111–6362

Soft Matter

www.softmatter.org

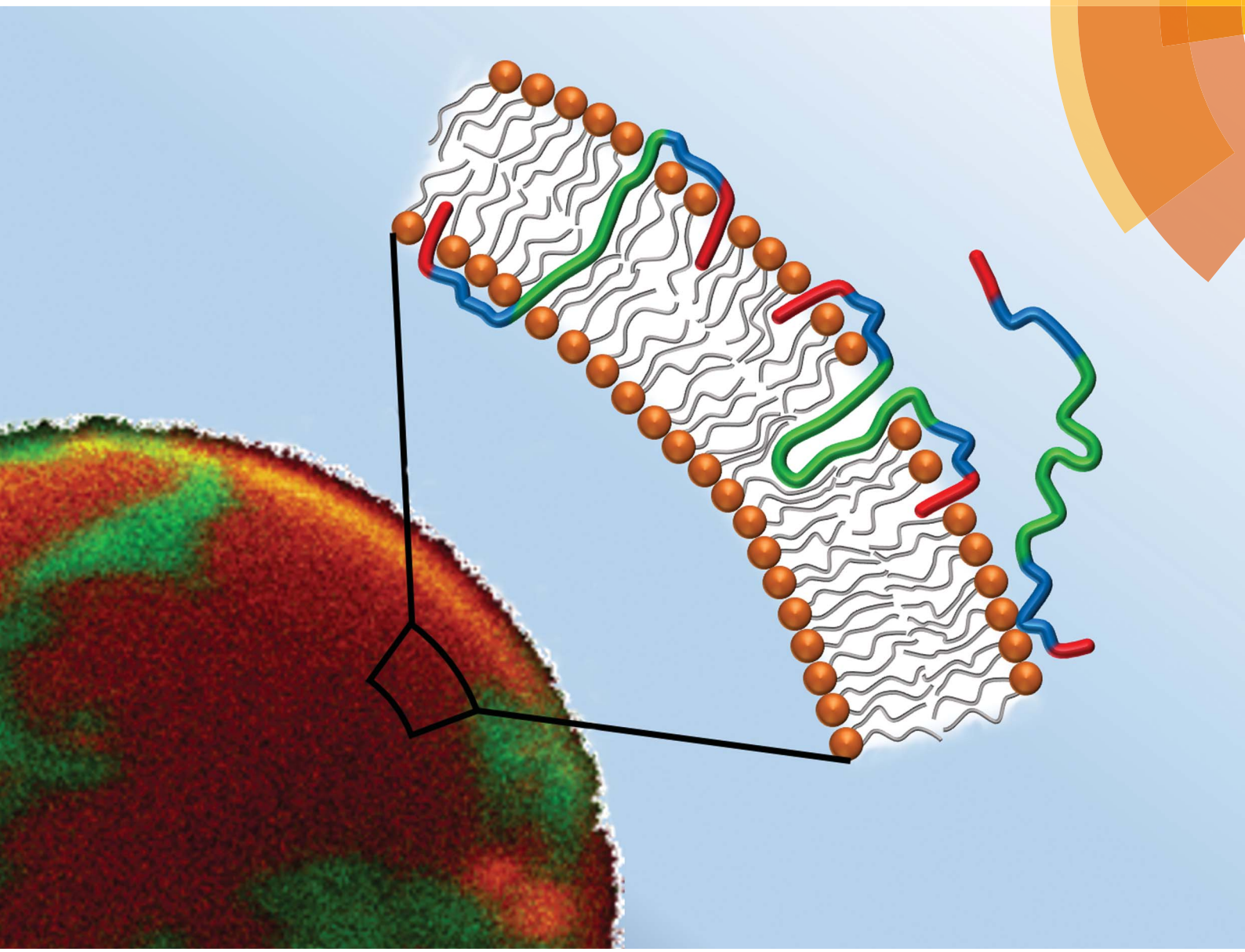

ISSN 1744-683X

ROYAL SOCIETY OF CHEMISTRY

PAPER
Christian Schwieger *et al.*
Binding of amphiphilic and triphilic block copolymers to lipid model membranes: the role of perfluorinated moieties

Soft Matter

PAPER

View Article Online
View Journal | View Issue

Cite this: *Soft Matter*, 2014, **10**, 6147

Binding of amphiphilic and triphilic block copolymers to lipid model membranes: the role of perfluorinated moieties

Christian Schwieger,*[a] Anja Achilles,[b] Sven Scholz,[a] Jan Rüger,[a] Kirsten Bacia,[c] Kay Saalwaechter,[b] Jörg Kressler[a] and Alfred Blume[a]

A novel class of symmetric amphi- and triphilic (hydrophilic, lipophilic, fluorophilic) block copolymers has been investigated with respect to their interactions with lipid membranes. The amphiphilic triblock copolymer has the structure $PGMA_{20}$-PPO_{34}-$PGMA_{20}$ (GP) and it becomes triphilic after attaching perfluoroalkyl moieties (F9) to either end which leads to F_9-$PGMA_{20}$-PPO_{34}-$PGMA_{20}$-F_9 (F-GP). The hydrophobic poly(propylene oxide) (PPO) block is sufficiently long to span a lipid bilayer. The poly(glycerol monomethacrylate) (PGMA) blocks have a high propensity for hydrogen bonding. The hydrophobic and lipophobic perfluoroalkyl moieties have the tendency to phase segregate in aqueous as well as in hydrocarbon environments. We performed differential scanning calorimetry (DSC) measurements on polymer bound lipid vesicles under systematic variation of the bilayer thickness, the nature of the lipid headgroup, and the polymer concentration. The vesicles were composed of phosphatidylcholines (DMPC, DPPC, DAPC, DSPC) or phosphatidylethanolamines (DMPE, DPPE, POPE). We showed that GP as well as F-GP binding have membrane stabilizing and destabilizing components. PPO and F9 blocks insert into the hydrophobic part of the membrane concomitantly with PGMA block adsorption to the lipid headgroup layer. The F9 chains act as additional membrane anchors. The insertion of the PPO blocks of both GP and F-GP could be proven by 2D-NOESY NMR spectroscopy. By fluorescence microscopy we show that F-GP binding increases the porosity of POPC giant unilamellar vesicles (GUVs), allowing the influx of water soluble dyes as well as the translocation of the complete triphilic polymer and its accumulation at the GUV surface. These results open a new route for the rational design of membrane systems with specific properties.

Received 16th April 2014
Accepted 3rd June 2014

DOI: 10.1039/c4sm00830h

www.rsc.org/softmatter

Introduction

Amphiphilic block copolymers have been shown in numerous studies to influence the properties and integrity of lipid membranes. Research in this field has been stimulated by their potential use in pharmaceutical and medical applications. Poloxamers (also known under the trade names Pluronics® or Synperonics®) are in this respect the most extensively studied block copolymers. They have a symmetric ABA architecture and consist of a hydrophobic poly(propylene oxide) (PPO) middle block, flanked by a hydrophilic poly(ethylene oxide) (PEO) block on either side. Depending on the length of the PPO and PEO blocks they show very different behaviour. On the one hand they have been shown to disturb the membrane integrity leading to an increased permeability and facilitated translocation of dyes[1] or drugs[2] across the membrane; on the other hand they can also act as membrane sealants, which reduce membrane leakage or even help to restore the permeation barrier of damaged membranes.[3] Both effects are of potential pharmaceutical interest, *e.g.* as chemo-sensitizer for drug uptake or as healing agent for injured cell membranes.[4,5] Key parameters that regulate the type of interaction are the hydrophilic/hydrophobic balance (HLB), *i.e.* the ratio of PPO and PEO block lengths[6] on the one hand and the absolute length of the PPO block on the other hand.[7] In general, a higher hydrophobicity leads to enhanced insertion of the copolymers into the membrane. The length of the hydrophobic block defines the pathway of hydrophobic insertion.[7,8] Copolymers with longer PPO chains can span the membrane, with their hydrophilic blocks being directed to either side of the bilayer. Copolymers with shorter PPO block insert only partially from one side.[8,9]

A sufficient hydrophilicity is necessary to render the polymers water soluble and to prevent a strong self-aggregation, *i.e.* micellization of the polymers in the aqueous phase. In case of poloxamers this hydrophilicity is imposed by the PEO blocks.

[a]*Institute of Chemistry, Martin Luther University Halle-Wittenberg, 06120 Halle (Saale), Germany. E-mail: christian.schwieger@chemie.uni-halle.de*
[b]*Institute of Physics, Martin Luther University Halle-Wittenberg, 06120 Halle (Saale), Germany*
[c]*ZIK HALOmem, Martin Luther University Halle-Wittenberg, 06120 Halle (Saale), Germany*

However, PEO interacts only marginally with the lipid bilayer[2] and counteracts the propensity of insertion. To overcome this drawback, it was proposed to substitute the PEO blocks by poly(glycerol monomethacrylate) (PGMA) blocks.[10,11] Due to the high propensity of PGMA to act as hydrogen bond donor and acceptor, the interaction with the lipid headgroups should be markedly increased. Moreover, the bulkiness of the PGMA side chains might increase the membrane disturbing effects, as it was reported for copolymers containing hyperbranched polyglycerols.[12] The self-aggregation behaviour of such amphiphilic PGMA-PPO-PGMA triblock copolymers in aqueous solution[11] as well as their behaviour at the air/water interface[13] and their interactions with lipid monolayers[14] have been studied before. It was shown that PGMA-PPO-PGMA inserts into lipid monolayers above the monolayer-bilayer equivalence pressure and affects the organization of the lipid molecules. We now present the first study on the interaction of these novel triblock copolymers with lipid bilayers, servings as model for biological membranes. The PPO block of the investigated copolymers has a degree of polymerization (DP) of 34 which is sufficient to potentially span a lipid bilayer. The PGMA blocks have each a DP of 20, which makes the polymers water soluble.

This triblock copolymer was investigated along with one of its derivatives, which was synthesized by terminally attaching perfluoroalkyl chains to both PGMA blocks.[15] The resulting polymer has the structure F_9-$PGMA_{20}$-PPO_{34}-$PGMA_{20}$-F_9, where F_9 stands for a perfluorononyl moiety. The chemical structures of both polymers under investigation along with their approximate contour block length are given in Fig. 1. Throughout this report the non-fluorinated triblock copolymer will be abbreviated with GP and the fluorinated derivative with F-GP. The fluorinated chains are hydrophobic, but not lipophilic,[16] *i.e.* they are fluorophilic and not miscible with *n*-alkanes (C_6 and above) and separate into an own phase. Therefore, the fluorinated copolymers are called triphilic or polyphilic.[17] This triphilicity leads to interesting self-aggregation in aqueous environment into multi-compartment micelles.[18,19] It might also lead to interesting new structures of the inserted triphilic polymer within the lipid bilayers. It is one aim of this work to investigate the influence of the fluorinated chains on the interaction of the block copolymers with lipid bilayers.

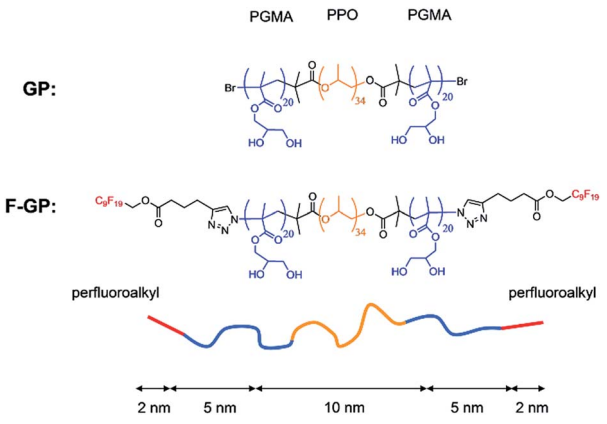

Fig. 1 Structures of the studied block copolymers GP and F-GP and schematic representation of a polymer chain with its hydrophobic (yellow), hydrophilic (blue) and fluorophilic (red) building blocks and their approximate contour lengths in fully stretched all-trans conformation.

The influence of GP and F-GP adsorption on the properties of lipid bilayers was investigated by differential scanning calorimetry (DSC) experiments. DSC monitors the gel to liquid phase transition temperature (T_m) of the membranes. T_m is a thermodynamic property that is influenced by any changes in the free energy of the gel or liquid crystalline phase of the bilayer. Therefore, it is sensitive to polymer adsorption and/or insertion which lead to changes in enthalpy and/or entropy of the system. However, systematic experiments and thorough analyses are necessary to conclude on a binding situation. Some DSC studies have been performed on the interaction of poloxamers with lipid membranes with different, partly conflicting results.[7,9,20–22] This might be due to the variety of studied poloxamers but also to the difficulty to disentangle the possible effects on T_m. In this study systematic variation of bilayer thickness, nature of the lipid headgroup and polymer concentration allowed us to unravel different modes of interaction between the polymers and the lipid membrane and their different effects on T_m. In addition, we used 2D-NOESY NMR spectroscopy to investigate the insertion of the block copolymers into the bilayer by monitoring the spatial proximity of lipid acyl chains and PPO units. On a larger length scale we used fluorescence microscopy to show the effect of GP and F-GP binding on the membrane integrity. We examined the capacity of both polymers to facilitate dye influx into giant unilamellar vesicles (GUVs) as well as the ability of the complete copolymers to translocate across the bilayer.

The combination of these methods together with the systematic variation of the experimental parameters give a comprehensive view of the way the PGMA containing copolymers bind to lipid membranes and on the influence of the addition of fluorinated moieties to the chain ends.

Materials and methods

Materials

Lipids. 1,2-Dimyristoyl-*sn*-glycero-3-phosphocholine (DMPC), 1,2-dipalmitoyl-*sn*-glycero-3-phosphocholine (DPPC), 1,2-dimyristoyl-*sn*-glycero-3-phosphoethanolamine (DMPE) and 1,2-dipalmitoyl-*sn*-glycero-3-phosphoethanolamine (DPPE) were bought from Genyzme (Neu-Isenburg, Germany). 1,2-Distearoyl-*sn*-glycero-3-phosphocholine (DSPC) was a gift from Nattermann Phospholipid GmbH (Cologne, Germany) and 1,2-diarachidoyl-*sn*-glycero-3-phosphocholine (DAPC) as well as 1-palmitoyl-2-oleoyl-*sn*-glycero-3-phosphocholine (POPC) were bought from Sigma Aldrich (Steinheim, Germany). All lipids were used without further purification. 1-Palmitoyl-2-oleoyl-*sn*-glycero-3-phosphoethanolamine (POPE) was bought from Avanti Polar Lipids (Alabaster, AL, USA).

Polymers. The triblock copolymer $PGMA_{20}$-PPO_{34}-$PGMA_{20}$ (GP) and perfluoroalkyl end-capped triblock copolymer F_9-$PGMA_{20}$-PPO_{34}-$PGMA_{20}$-F_9 (F-GP) were synthesized according to the procedure described in previous publications.[11,15] Their

average mol mass ($M_{GP} = 8555$ g mol^{-1}; $M_{F\text{-}GP} = 9830$ g mol^{-1}), chain lengths (given by the subscripts) and polydispersity (PDI = 1.2), were determined by ^{1}H NMR and GPC. Both polymers were synthesized from the same batch, *i.e.* block lengths and polydispersities are identical.

Rhodamine-conjugated copolymers. Tetramethyl-rhodamine (TMR)-conjugates of both GP and F-GP were synthesized as follows: the respective block copolymer (30 mg) was dissolved in water-free DMF (10 mL, Sigma Aldrich), stored under nitrogen and heated to 85 °C on a silicon bath. A solution of TMR-5-carbonyl azide (2 mg, Invitrogen) in DMF (20 mL) was added dropwise over a time period of 5 h under nitrogen. The resulting reaction mixture was kept at 85 °C for 24 h. To remove unconjugated dye, the reaction mixture was placed in a dialysis bag (Spectra/Por, Spectrum Laboratories Inc., MWCO = 1000 Da) and dialyzed against DMF for 4 days. Both, the dialysis bag and the solvent were renewed two times per day. Afterwards the solution was dialyzed against deionized water until no fluorescence signal due to remaining unconjugated dye in the solution was detectable. Again, both dialysis bag and the solvent were changed twice a day. Finally, the aqueous solution was freeze-dried.

Other compounds. The dyes TMR, BODIPY® and Alexa Fluor® 488 hydrazide were bought from Invitrogen (Life Technologies, Darmstadt, Germany). Organic solvents were used in HPLC grade. All experiments were performed in ultrapure water (MiliQ Advantage A10, Merck Millipore, Billerica, MA) with a conductivity lower than 0.55 μS cm^{-1}.

Methods

Vesicle preparation. For DSC experiments large unilamellar vesicles (LUVs) were prepared as follows: lipids were dispersed in aqueous solution by heating above the phase transition temperature and vortexing. Vesicles were then sized by extrusion through a 100 nm polycarbonate membrane at 20 °C above the respective transition temperature, using a Mini-Extruder from Avanti Polar Lipids Inc. Vesicle size was determined by dynamic light scattering using an ALV-NIBS/HPPS spectrometer (ALV-Laser Vertriebsgesellschaft m.b.H., Langen, Germany).

For the CLSM experiments giant unilamellar vesicles (GUVs) were prepared by a modified electroformation method. POPC was dissolved in chloroform at a total concentration of 10 mg mL^{-1}. For the polymer co-localization experiments the membrane label BODIPY (0.5 mol%) was added. After manual spreading of this solution onto two indium-tin-oxide (ITO) coated glass slides (GeSiM, Großerkmannsdorf, Germany) the lipid film was dried at 60 °C. Both slides separated by a 3 mm thick silicon spacer and held together with office clips were used to form a chamber that was filled with sucrose solution (530 mOsmol kg^{-1}). *Via* copper conductive tape (3M, SPI supplies) the slides were connected to a pulse generator (Conrad, Germany) and a 3 V, 10 Hz sinusoidal voltage was applied for 5 h. The formed GUVs were collected overnight by sedimentation in an iso-osmolar glucose solution.

DSC. Differential Scanning Calorimetry (DSC) was performed with a Microcal VP-DSC (MicroCal Inc., Northhampton, USA). In all experiments we used a heating rate of 1 °C min^{-1} and a time resolution of 4 s. Aqueous lipid vesicle suspensions (LUVs) and polymer solutions were prepared separately and mixed directly before measurement. The lipid concentration was always 1 mmol L^{-1}. The polymer concentration was adjusted to give the desired molar mixing ratio. Reference was always degassed ultrapure water. At least three up- and down scans were performed for each sample to prove the reproducibility. The presented curves originate from the second heating scan. The third heating scan was always identical to the second one. After subtraction of a water/water reference measurement an additional cubic baseline was subtracted from all measured curves. Data processing was done with the DSC module for ORIGIN software supplied by MicroCal Inc.

CLSM. Confocal laser scanning microscopy (CLSM) images were obtained on a Zeiss LSM 710 inverted microscope (Carl Zeiss Microimaging, Jena, Germany) using a LD C-Apochromat 40×/1.1 N.A. water immersion objective. Membrane staining BODIPY was excited with an argon ion laser at 633 nm. The polymer linked rhodamine label or the free Alexa488 dye were simultaneously excited with a HeNe laser at 488 nm.

For the dye influx experiments 20 μL of the copolymer solution (0.8 mmol L^{-1} GP; 0.9 mmol L^{-1} F-GP) and 4 μL of an aqueous dye solution (Alexa Fluor® 488 hydrazide, 500 nmol L^{-1}) were pre-mixed in a 96 well plate. 1 μL of the respective GUV suspension was then carefully injected from above and allowed to settle to the well's ground. To prevent osmotic pressure differences, all solutions contained iso-osmolar amounts of glucose. After addition of the GUV suspension the well plate was immediately mounted on the microscope. After focusing on selected GUVs, images were recorded in a time series with a camera exposure time of 300 ms. Due to this procedure there is a lag time between mixing of the GUVs with the polymer solution and the beginning of the time series of maximal 10 s. The recorded images were processed with the ZEN microscope software (Carl Zeiss Microimaging). To evaluate the amount of dye influx, integral fluorescence intensities of selected regions of interest were determined and normalized to the average intensity of the respective image.

Colocalization experiments of membrane stained GUVs and rhodamine-labelled polymer were performed in an analogous manner.

NMR. To investigate the interaction of polymer samples with lipid molecules, solid-state magic-angle spinning (MAS) nuclear magnetic resonance (NMR) experiments were performed. A suitable NMR method to prove the spatial proximity between two nuclei is the 2D-NOESY-experiment,[23–25] for which we have used a three-pulse sequence in phase-sensitive mode as described earlier.[26]

In the resulting two-dimensional spectrum $S(\omega_1,\omega_2)$, ω_1 characterizes the resonance frequency of a given nucleus before, and ω_2 the frequency after the mixing time t_m, *i.e.* after a possible polarization transfer. If a polarization transfer occurred during t_m, a crosspeak will appear in the correlation spectrum arising from a spatial proximity between the nuclei with the respective chemical shifts. However, due to complex dependence of the cross-correlation on the distance between

the nuclei and their dynamics, the NOESY-experiment only yields qualitative information on possibly transient contacts.

For the NMR measurements the samples were prepared directly within the NMR rotor by loosely filling it with the sample mixture (DMPC and polymer), adding 50 wt% of D_2O afterwards and letting it equilibrate at a temperature above the main phase transition of the lipid in order to obtain a homogeneous suspension. All NMR experiments were carried out on a Bruker Avance III 400 spectrometer with resonance frequencies of 400.03 MHz for protons, using a double-resonance 4 mm probe at a rotation frequency of 4 kHz. The 90° proton pulse was 3 μs, the mixing time was set to 200 ms and a total of 512 t_1 increments were acquired with 16 scans for each increment and a relaxation delay of 1 s. For best spectral resolution, the samples were investigated in the L_α phase and hence heated to a temperature of 40 °C.

Results and discussion

DSC: influence of polymer binding on the transition temperatures of lipid membranes

Using DSC measurements the influence of the polymers on the gel to liquid crystalline ($L_{\beta'} \rightarrow L_\alpha$) phase transition of lipid membranes composed of phosphatidylcholines can be monitored. This transition is a cooperative first order transition and gives a peak in the $C_p = f(T)$ thermogram, where the integral of the peak corresponds to the phase transition enthalpy and the width is a measure for the cooperativity (the narrower, the more cooperative). The maximum of the DSC trace is the main transition temperature (T_m) of the lipid membrane.

T_m is sensitive to interactions on the membrane surface and/or insertion of hydrophobic substances into the hydrophobic part of the membrane. T_m increases when the interaction leads to a screening of headgroup charges, a displacement of hydration water from the hydrophilic membrane layer,[27,28] or hydrogen bond formation between the headgroups.[29,30] When hydrophobic molecules or moieties insert into the hydrophobic layer of the membrane T_m decreases due to a perturbation of the chain packing.[29–32]

The copolymers under investigation, being amphiphilic (GP) or triphilic (F-GP), have the potential to interact with the hydrophilic headgroup layer *via* the PGMA blocks and with the hydrophobic acyl chain layer *via* the PPO block.[8,33] Due to their hydrophobicity also the perfluoro segments have the tendency to partition into the hydrophobic membrane layer. However, their lipophobic nature might lead to a segregation of inserted fluorinated moieties within the membrane. An influence on T_m would depend on the nature and the balance of the interactions between the lipids and the copolymers. Thus, the change in T_m is a marker for the type of interaction that occurs in this system and about the influence of end-cap fluorination of the copolymers.

To decipher the possible interactions we performed a number of experiments under systematic variation of (i) the type of polymer, (ii) the added polymer concentration, (iii) the hydrophobic thickness of the membrane and (iv) the nature of the lipid headgroup.

Influence of lipid chain length. The first set of DSC experiments was performed with vesicles of saturated diacyl-phosphatidylcholines (PCs), which are abundant in biological membranes and belong to the most studied lipids. The copolymers were always added to preformed vesicles, so that the first interaction occurs with the outer monolayer of the lipid vesicle. The polymer concentration was varied from 0.2 to 10 mol% with respect to the total amount of lipids. As the lipid concentration was set to 1 mmol L^{-1} for all DSC experiments this corresponds to absolute polymer concentrations of 2 to 100 μmol L^{-1}. The interaction was studied for lipids with increasing acyl chain length, *i.e.* DMPC, DPPC, DSPC and DAPC, which possess 14, 16, 18 and 20 carbon atoms per acyl chain, respectively. This increasing acyl chain length increases the hydrophobic thickness of the fluid bilayer from approximately 2.5 nm for DMPC[34,35] to 3.2 nm for DAPC.[36] The increase in hydrophobicity and van der Waals interactions lead to a stabilization of the gel phases and to an increase in T_m from 24 °C for DMPC up to 65 °C for DAPC. The phase transitions of the pure lipid membranes are represented by the lowest black curves in Fig. 2A–D. The maxima of the recorded transition peaks correspond well to T_m values reported in literature.[32,37,38] The influence of polymer addition to the lipid vesicles is different depending on the type of polymer, the type of lipid and the molar mixing ratio.

Fig. 2A summarizes the DSC scans of the second heating of DMPC–copolymer mixtures. Already a very low polymer content of 0.2 mol% leads to a shift of T_m to lower values ($\Delta T_m < 0$). This shift gets systematically larger as the copolymer content increases, leading to a 1 °C downshift at a GP content of 10% and even a 4 °C downshift for the same F-GP content. From Fig. 2A it becomes evident that F-GP binding (red curves) has a stronger influence on the DMPC phase transition than GP-binding (blue curves). The shift of T_m to lower temperature indicates the insertion of the copolymers into the hydrophobic part of the lipid bilayer. Probably, the hydrophobic PPO block inserts into the acyl chain region of the membrane perturbing the acyl chain packing, as it was also postulated for the related poloxamers.[8] The fact that F-GP decreases T_m more than GP shows that not only the PPO block but also the terminal perfluoroalkyl chains insert into the membrane. This confirms that the hydrophobic nature of the perfluoroalkyl chains dominates their lipophobic nature. For transitions of F-GP–DMPC mixtures with low F-GP content no single peaks are observed but additional minor transition components emerge on the low temperature side of the main peak. With higher F-GP content, a broad transition at higher temperature develops which is clearly separated from the transition at lower temperature. This biphasic transition is an indication for a partial phase separation into ordered domains of different compositions. Possibly, there are polymer rich regions in the membrane where the acyl chain melting is retarded either by strong headgroup interactions or by an order that is conferred by inserted, rigid fluorocarbon chains.

Whatever the exact reason, it must be due to the presence of the fluorinated moieties in the system, as it is not observed for the non-fluorinated triblock copolymer (GP).

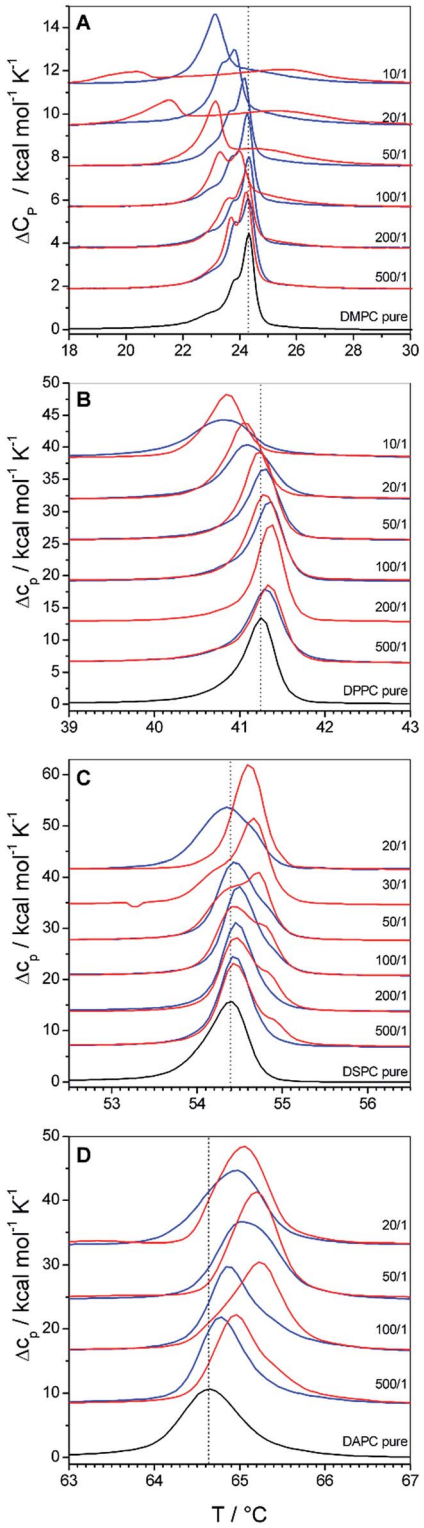

Fig. 2 DSC thermograms of polymer bound lipid vesicles prepared from (A) DMPC, (B) DPPC, (C) DSPC and (D) DAPC. Black traces represent the phase transition of the pure lipid vesicles, blue traces their mixtures with GP and red traces their mixtures with F-GP. The lipid/polymer molar mixing ratio is given in the figure. Dotted lines are drawn at T_m of the pure lipid membranes.

In Fig. 2B we show the influence of copolymer binding on the phase transition of DPPC vesicles. Even though DMPC and DPPC are homologous phospholipids which differ only in the length of their acyl chains, the influence of copolymer binding on their phase transitions is surprisingly different: at low polymer contents (0.2 to 1 mol%) T_m of DPPC is shifted to higher temperatures ($\Delta T_m > 0$). Only at higher polymer content (>1 mol%) T_m decreases as it was observed for DMPC membranes. The ability of the polymers to induce both, an upshift and a downshift of T_m shows that the insertion of the hydrophobic polymer block and the fluorinated chain in the case of F-GP is not the only mode of interaction. The increase of T_m indicates that also polar interactions occur between the lipid headgroups and the hydrophilic moieties of the copolymers, *i.e.* the PGMA blocks. The overall effect on T_m is a result of the delicate balance of hydrophobic and polar interactions, which occur concurrently but influence the phase transition in an opposite manner. The compensation of both counteracting effects explains that the changes in T_m are relatively small in absolute values. A similar balance of T_m increasing and T_m decreasing effects was observed before for binding of polyelectrolytes to lipid membranes.[39]

The balance of hydrophobic effects and polar interactions is concentration dependent. At low polymer contents polar interactions dominate the influence on T_m and over-compensate the effect of perturbation of chain packing by insertion of the hydrophobic polymer block into the acyl chain region. At higher polymer content it is well imaginable that the hydrophilic polymer blocks are stretched into the surrounding aqueous solution because of crowding effects. As a consequence, the polar interactions between the PGMA block and the bilayer surface are reduced leading to a decrease in T_m due to perturbations of chain packing. A concentration dependent change in binding mechanism was also predicted by molecular dynamics simulations for poloxamer binding to lipid membranes[8] and a concentration dependent change in the sign of ΔT_m was also shown for poloxamer binding to DPPC vesicles.[9] The difference in the influence of GP and F-GP binding on T_m of DPPC membranes seems to be small. However, slightly narrower transitions are observed for mixtures with F-GP.

A further increase in the hydrophobic thickness of the membrane leads to the transitions depicted in Fig. 2C for DSPC (18 C-atoms per acyl chain) and Fig. 2D for DAPC (20 C-atoms per acyl chain). Copolymer addition to these thicker membranes does not lead to a T_m decrease and ΔT_m stays positive at all concentrations and for both copolymers. The increase is more pronounced for DAPC than for DSPC and more pronounced for addition of F-GP compared to GP. For both types of membranes and for both types of polymers the concentration dependence that leads to a maximum in ΔT_m at intermediate polymer contents is still visible. This shows that both, insertion into the hydrophobic membrane layer and hydrophilic interactions in the headgroup layer still compete in their effect on T_m. However, for these thicker membranes the polar interactions always dominate the effect on T_m, leading to an over-all stabilization of the membranes gel phases. The increase in the lipids acyl chain length increases

the van-der-Waals interactions in the hydrophobic membrane layer, which is reflected by the increasing transition temperatures of the pure membranes (black traces). The perturbation of the acyl chain order which is exerted by the insertion of PPO-blocks and perfluorocarbon chains is the less pronounced the more stable this layer is. Thus, the effect of PPO/perfluorocarbon insertion on T_m decreases with increasing bilayer thickness. Simultaneously, the effect on the headgroup layer is always the same as it does not depend on the bilayer thickness. In combination, this leads to the observed increasing influence of the polar headgroup interaction on T_m with increasing bilayer thickness.

The comparison of the effects of GP and F-GP on DAPC and DSPC shows again that both copolymers have qualitatively the same effects on T_m but that the addition of perfluorinated chains leads to an increase in its magnitude. The addition of perfluorinated segments increases on the one hand the downshift of T_m (for DMPC) and on the other hand the upshift of T_m (for DAPC and DSPC). This indicates that the addition of the two perfluorinated moieties to the ends of each polymer chain leads to an increase in the apparent binding constant, thus amplifying both hydrophobic and polar interactions at the membrane surface. The perfluoroalkyl chains thus function as additional membrane anchors due to their high hydrophobicity.

Fig. 3 summarizes the effects of GP and F-GP binding on T_m of the different examined PC membranes. The following systematic trends can be extracted:

i. Stabilization ($\Delta T_m > 0$) and destabilization ($\Delta T_m < 0$) of the membrane are possible. The overall effect is a superposition of both.

ii. The effect on T_m is concentration dependent, with a maximum of ΔT_m at intermediate concentrations (about 1 mol% polymer).

iii. Sign and absolute value of ΔT_m depend on the hydrophobic thickness of the membrane. The higher the membrane thickness, the less important is the effect of perturbation of acyl chain packing and the more positive is ΔT_m.

iv. Addition of perfluorinated moieties at the chain ends of the polymers leads to an amplification of all effects.

Headgroup variation. The fact that the influence of the polymers on T_m is modulated by the hydrophobic thickness of the membrane unambiguously shows that partial insertion of the polymer into the membrane takes place. The existence of polar interactions with the headgroup layer was concluded from the positive ΔT_m that was detected under certain conditions for PC membranes. To directly show the contribution of headgroup interactions to copolymer binding we varied also the chemical structure of the lipid headgroup. Replacement of the three methyl groups of the choline in the PC headgroup by hydrogen atoms leads to the phosphatidylethanolamine (PE) headgroup. Both headgroups, PC and PE, are zwitterionic, *i.e.* electrically neutral. However, the PE headgroup is smaller and has a higher propensity for intermolecular hydrogen bonding.[40] The hydrogen bonding between neighbouring PE headgroups leads to a stabilization of the membrane and to an increase in the phase transition temperature as compared to PCs of equal acyl

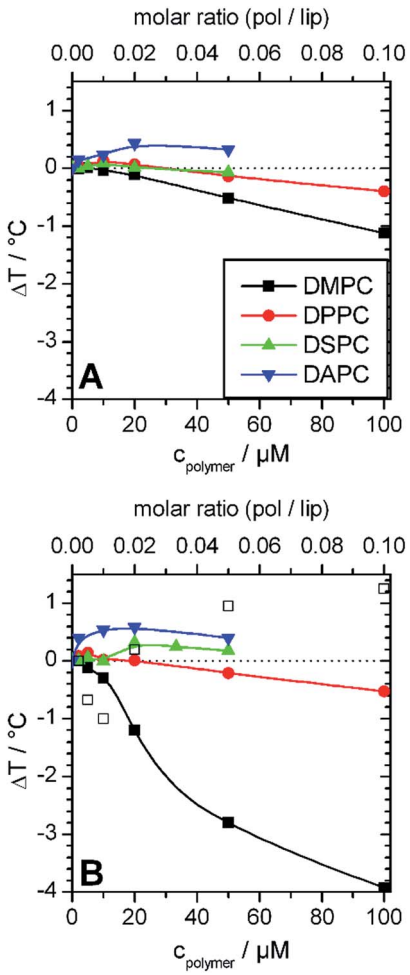

Fig. 3 Change of main transition temperatures of the lipid membranes prepared from DMPC (black), DPPC (red) DSPC (green), DAPC (blue) after addition of different amounts of (A) GP and (B) F-GP. The lipid concentration was always 1 mmol L^{-1}. In (B) major (solid symbol) and minor (open symbol) transition components are shown for DMPC, where *major* refers to the transition component with the maximal c_p value and *minor* to shoulders or transition peaks with lower c_p values (see Fig. 2A). Copolymer/lipid molar ratios are presented on the top *x*-axes. The inserted lines are drawn to guide the eyes.

chain length.[41,42] This can be observed in Fig. 4A and B, which show the phase transitions of DMPE and DPPE, respectively. The determined T_m values of 49.4 °C and 63.4 °C (black traces in Fig. 4) correspond well to values reported in literature.[43] In Fig. 4A the influence of copolymer addition on the phase transition of DMPE is shown. The absolute effect on T_m is quite small, but a slight increase is observed upon addition of GP as well as upon addition of F-GP at almost all tested concentrations. Also the copolymer addition to DPPE membranes results in a slight increase in T_m (Fig. 4B). The values of ΔT_m depend again on the concentration and the type of polymer (see Fig. 5). For DPPE membranes there is a maximum in ΔT_m at intermediate F-GP concentrations (2 mol%) (Fig. 5B).

These effects are small, but become interesting in comparison with the corresponding data of copolymer/PC membrane

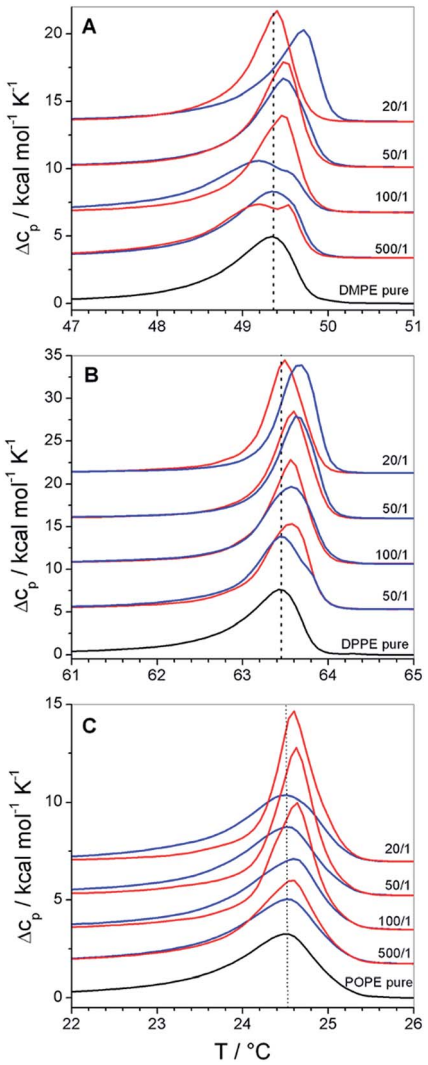

Fig. 4 DSC thermograms of polymer bound lipid vesicles prepared from (A) DMPE, (B) DPPE and (C) POPE. Black traces represent the phase transition of the pure lipid vesicles, blue traces their mixtures with GP and red traces their mixtures with F-GP. The lipid/polymer molar mixing ratio is given in the figure. Dotted lines are drawn at T_m of the pure lipid membranes. The lipid concentration is always 1 mmol L^{-1}.

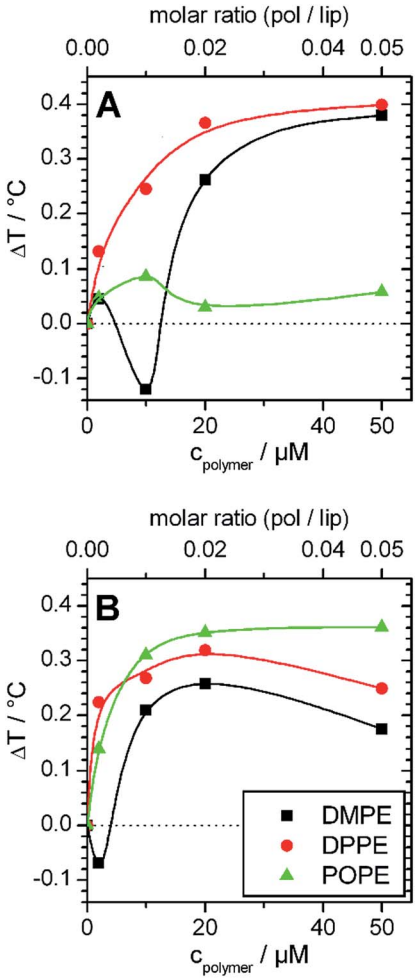

Fig. 5 Change of main transition temperatures of lipid membranes prepared from DMPE (black), DPPE (red) and POPE (green) after addition of different amounts of (A) GP and (B) F-GP. The lipid concentration is always 1 mmol L^{-1}. The temperature where half of the transition enthalpy was consumed was interpreted as transition temperature. The inserted lines are drawn to guide the eyes.

aggregates, were the T_m shift was negative (see Fig. 2A, 2B and 3). The only difference between DMPC and DMPE as well as between DPPC and DPPE is the chemical structure of the headgroup. Thus, the different influence on T_m must be due to polar interactions between the copolymers and the headgroups. Therefore, the presented results are a direct proof for the existence of interactions between the PGMA blocks of the polymer and the lipid headgroups. The fact that the polymer binding induces a more positive T_m shift for PE membranes than for PC membranes of equal chain length indicates that polar interactions between the polymers and the PE headgroup are more dominant. This is due to the ability of PE to act as both, as hydrogen bond donor and acceptor.[40] High propensities for hydrogen binding are also known for PGMA.[14,18] Thus, a contribution of hydrogen bonds between the PGMA blocks of the polymers and the PE headgroup to the polar interactions can be assumed.

Temperature dependence. The above considerations are based on the assumption that the absolute temperature does not influence the interaction strength. However, we know that the temperature has an influence on the properties of the copolymers in aqueous solution. The solubility of the PGMA block is not temperature dependent[11,44] but the PPO block has an LCST at about 13 °C and becomes more hydrophobic with increasing temperature.[7,18] This leads to a temperature dependent self-aggregation process.[11,18,19,45] For the related poloxamer copolymers it is known that there is a critical micellization temperature (cmt).[46] Below the cmt poloxamers are dissolved as unimers in water. Above the cmt, poloxamers form micelles with segregated PPO cores. Interactions of lipid membranes with poloxamer depend on the state of their aggregation.[20] For the PGMA containing block copolymers, there is a wide temperature and concentration range of unimer/unimer-

aggregate/micelle coexistence.[11,18,19] Therefore, the question remains whether GP and/or F-GP interactions with lipid membranes depend on temperature. Is the more positive ΔT_m for PE membranes due to their higher values of T_m as compared to PC membranes? To answer this question we performed experiments with POPE membranes, which have a gel to liquid-crystalline phase transition temperature that is comparable to that of DMPC (*ca.* 24 °C). The results are shown in Fig. 4C and 5 (green traces). GP as well as F-GP addition to POPE increase T_m at all tested concentrations. Thus, the effect is similar to the effect that the polymer binding has on DMPE and DPPE membranes, which have a higher transition temperature. Compared to the effect of copolymer binding to DMPC membranes, the effects are quite different. Therefore, we conclude that the upshift of T_m after copolymer binding to PE membranes is indeed due to the modified headgroup interactions and not an effect of the absolute temperature.

Moreover, it can be seen that POPE/copolymer transitions which are depicted in Fig. 4C are always unimodal and highly cooperative. It means that the bimodal transitions which were detected for the DMPC–F-GP mixtures in the same temperature range are not due to any change in the aggregation state of the copolymer.

NMR: localization of the PPO block

From DSC measurements at different conditions we concluded that the hydrophobic parts of the polymer insert into the lipid bilayer. To be able to observe more directly the localization the copolymer within the lipid membrane, we performed solid state magic angle spinning (MAS) NMR spectroscopy.

Taking advantage of the high-resolution conditions provided by MAS solid-state NMR, the (temporary) spatial proximity of nuclei can be elucidated by means of the 2D-NOESY experiment.[47] This experiment can give answers to the question whether there is at least a temporary close proximity between the protons of the lipid molecules and those of the polymer molecules. This would allow to conclude on the depth of penetration of the polymer molecules into the lipid bilayer.

All experiments were performed on DMPC membranes in the L_α-phase, because gel phase membranes do not yield a sufficient spectral resolution for a 2D-NOESY analysis. In Fig. 6 the proton NMR spectrum of the mixture of DMPC and F-GP (5 mol%) recorded at a spinning speed of 4 kHz is shown. Due to many different proton types in the sample and the narrow chemical shift range, most of the polymer resonances overlay with resonances of the lipid. The only isolated resonance from the polymer is the signal of the PPO methyl group at a chemical shift value of approximately 1.1 ppm. Thus, information on the proximity of the PPO methyl group to nuclei of the lipid molecules can be obtained from crosspeaks between this polymer resonance and lipid resonances.

In Fig. 7 a close-up of the region of interest of the full 2D-NOESY spectrum is depicted for the mixture of DMPC with both polymers (Fig. 7A: GP, Fig. 7B: F-GP). In both spectra an off-diagonal signal is clearly detectable for the PPO methyl group and the $(CH_2)_{4\text{-}13}$ signal of the lipid acyl chains. To illustrate this in more detail, a slice through the PPO–methyl signal at

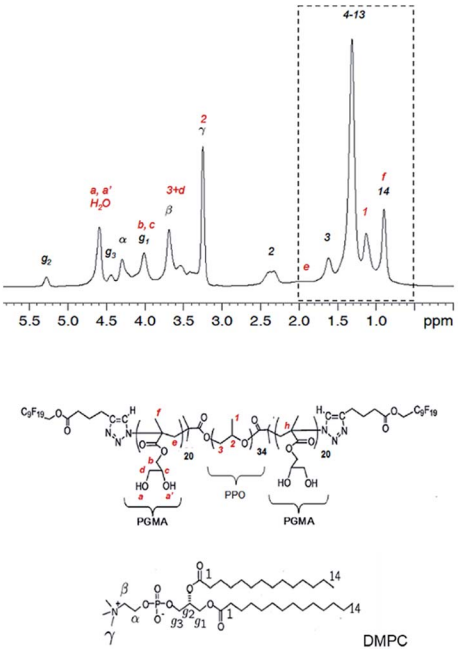

Fig. 6 ^{1}H NMR spectrum of the mixture of DMPC with F-GP (5 mol%) and structures of the molecules including assignment of the ^{1}H resonances. Peaks labelled in red originate from the polymer and peaks labelled in black originate from lipid resonances. The region of the spectrum inside the dashed box is evaluated in a 2D-NOESY experiment (see Fig. 7).

approximately 1.1 ppm in the ω_1 – dimension is shown in each of the spectra. The strong peak corresponds to the PPO–methyl resonance on the diagonal. To the left of this peak a small signal shows up at the chemical shift of the methylene groups of the lipid acyl chain (*ca.* 1.3 ppm), revealing that the corresponding nuclei exchanged magnetization during the mixing period. These crosspeaks confirm the insertion and mixing of the polymer molecules into the lipid bilayer. The crosspeaks are only of relatively small intensity, which is likely due to only weak and rather transient contacts in the fluid bilayers. Whether the polarization transfer occurs *via* an actual cross-relaxation (NOE) effect caused by rapidly fluctuating dipole–dipole couplings, or *via* spin diffusion caused by weak residual quasi-static couplings is not clear.[48,49] At any rate, the observed temporarily close molecular contacts between the hydrophobic groups of the lipid (acyl chains) and the hydrophobic block of the polymers (PPO) leads to the conclusion that the polymer is not only adsorbed onto the surface but is indeed inserted into the lipid membrane to a significant degree. This finding confirms the conclusions drawn from the DSC experiments.

The fraction of inserted polymer can also be estimated from a detailed study of residual dipole–dipole couplings within the PPO-chains as arising from pronounced anisotropic dynamics, as will be reported shortly.

CLSM: membrane integrity and pore formation

After having evidence that both, GP and F-GP insert into the hydrophobic part of the lipid bilayer the question arises to

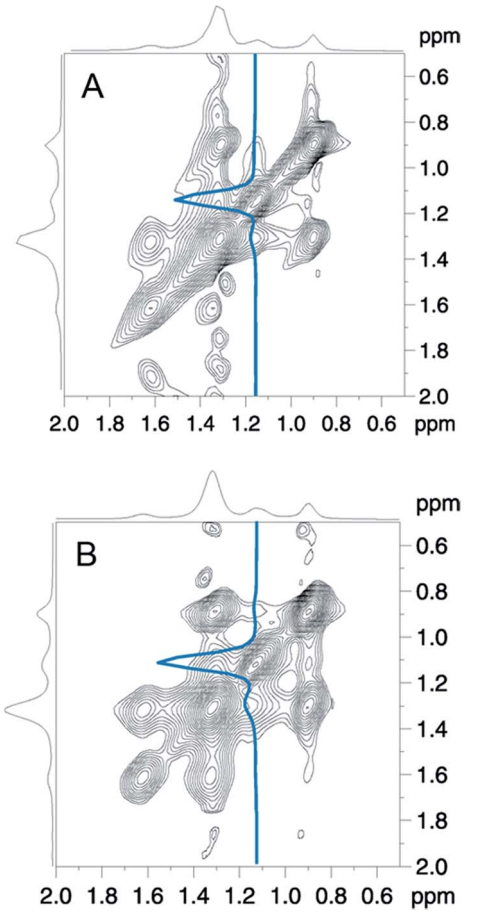

Fig. 7 2D-NOESY-spectra of DMPC mixed with (A) GP and (B) F-GP polymer (both 5 mol%) measured at 40 °C. The base level of the counter plots is set to 5% of the highest intensity. The blue lines represent slices at the position of the PPO–methyl resonance in the ω_1 – dimension.

which extent the membrane integrity is perturbed by this insertion. The questions whether the barrier function of the membrane is maintained, whether the copolymer insertion leads to pore formation or membrane defects, and whether the polymer can translocate through the membrane into the inner volume of the vesicles are addressed by two types of fluorescence microscopy experiments performed with giant unilamellar vesicles (GUVs). The GUVs were formed from POPC by electro-swelling. As the phase transition temperature of POPC is at −3 °C (ref. 50) and all experiments were performed at room temperature the results allow conclusions on the interactions of the polymers with fluid membranes.

Dye influx. The first set of fluorescence experiments addressed the question whether the copolymer insertion leads to pore or defect formation. Preformed GUVs were injected into copolymer solutions that contained an additional water soluble dye (Alexa-Fluor 488). In case of copolymer insertion leading to pore formation this dye would flow into the aqueous lumen of the GUVs, otherwise the dye would stay outside the GUVs. The dye distribution was monitored by time dependent fluorescence microscopy. The results are shown in Fig. 8. The upper row represents the control experiments, *i.e.* experiments where no copolymer was present. For the controls, it can be seen that the interior of the liposomes does not fluoresce, *i.e.* the dye cannot significantly permeate through pure POPC GUVs during an observation time of 10 min.

The middle row of Fig. 8 represents a time series of images taken after the GUVs have been injected into a GP–dye mixture. To be able to identify the same GUV in the different images, selected GUVs are marked by a number. A low fluorescence intensity can be detected in the lumen of most, but not all, of the GUVs after mixing. The intensity is always lower inside the GUVs than outside, indicating that complete mixing of the two volumes did not occur. Moreover, there is no evolution of fluorescence intensity within the observation time of 10–15 minutes, *i.e.* no dye influx was observed after the lag time of the experiment. This suggests that some transient pores or defects formed upon mixing of the GUVs with the polymer solution within the lag time, which then healed after an equilibrium was reached.

The same experiment performed with the fluorinated copolymer (F-GP) yields the microscopic images depicted in the bottom row of Fig. 8. Some of the GUVs are already filled with dye when the first image was taken (*e.g.* GUV 4), which means that there is a rapid dye influx after mixing. Other GUVs fill within the time scale of the experiment (*e.g.* GUV 1 and GUV 3). This provides clear evidence that F-GP adsorption and insertion leads to the formation of stable hydrophilic pores or defects, which allow the water soluble dye to diffuse into the interior volume of the GUVs. The images show that the liposomes stay intact and do not disintegrate or form other structures after being injected into the polymer solution. The images also show that the permeation of the dye is quite inhomogeneous, *i.e.* dye-filled GUVs coexist with GUVs that still maintain their barrier function over the time scale of the experiment. This is very similar to what was observed for some pore forming peptides (PFPs) interacting with GUVs[51] and indicates that the leakage mechanism is "heterogeneous graded".[52] Some of the vesicles might also be permeabilized by the "all or none" mechanism (GUV 4).

For quantification of dye influx we integrated the fluorescence intensity of the lumen of some selected GUVs (marked by numbers in Fig. 8) at different times and normalized it to the average intensity of the respective image. The resulting normalized intensities of some GUVs of the control sample are shown in Fig. 9A. The results for GP and F-GP containing GUV suspensions are shown Fig. 9B and C, respectively. The images of the GUVs of the control sample shown in Fig. 9A confirm that the normalized intensity values are lower than 1 and do not change with time indicating that no dye influx occurs. In Fig. 9B it can be seen that the fluorescence intensity within the selected GP-bound GUVs is higher than in the control but does not increase within the timescale of the experiment (15 min). In contrast, Fig. 9C shows that the fluorescence intensity inside GUVs mixed with F-GP increases with time. However, the kinetics of dye influx is different for the individual GUVs. The content of GUV 4 already completely mixed with the bulk solution at the beginning of the image recording. This indicates that pores of different size and lifetimes are formed upon F-GP

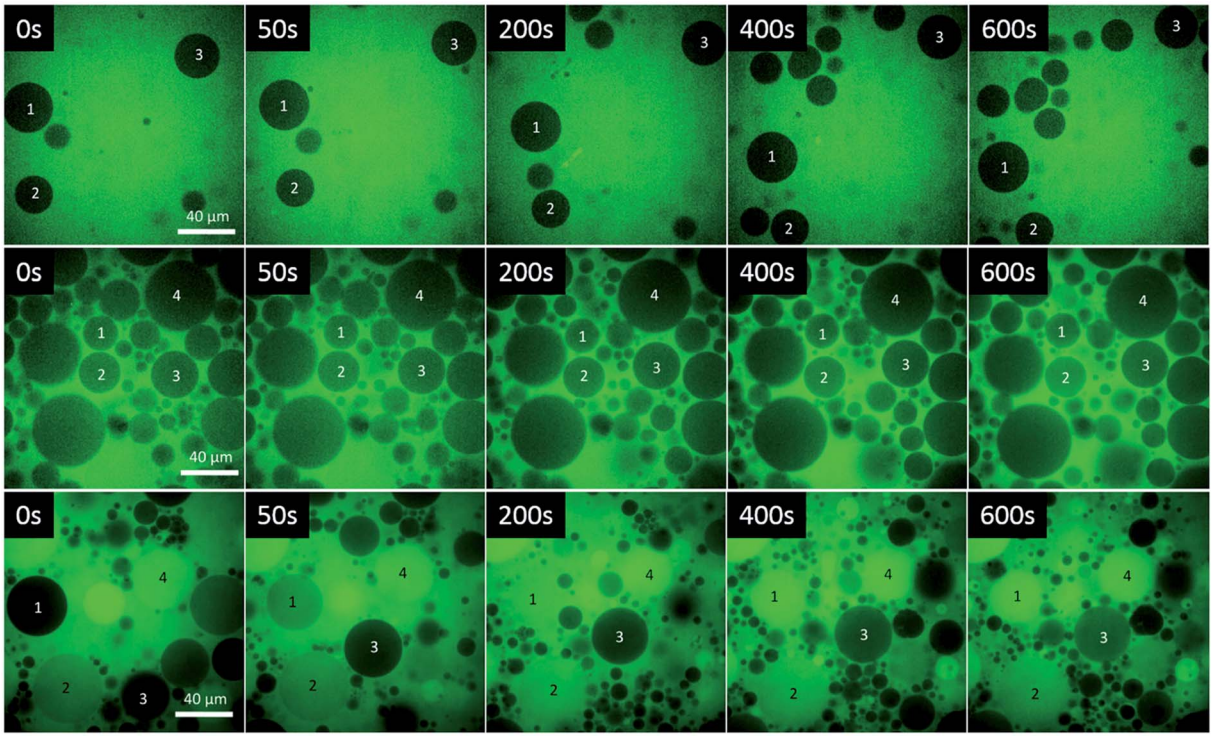

Fig. 8 Confocal laser scanning microscopy images of solutions containing the water soluble dye Alexa 488 and upper row: POPC GUVs; middle row: POPC GUVs + GP (8 mmoL L^{-1}) and lower row: POPC GUVs + F-GP (7.1 mmoL L^{-1}) at different time intervals after injecting the GUVs to the other components. The indicated times are times after the beginning of the microscopy. There is a small lag time between the GUV/polymer mixing and the begin of the microscopy of approximately 10 s.

binding to POPC vesicles and that the sample is not in a thermodynamic equilibrium at the end of the experiment.

The different dye influx kinetics of GP and F-GP containing samples reveals a clear influence of the perfluoroalkyl moieties. In the case of GP binding, the permeabilization is only minute and transient and is followed by resealing of the membrane once the equilibrium is reached. In the case of F-GP binding pores and/or defects are more stable and heterogeneous. An equilibrium is not reached within the time of the experiments. This might be due to a more complex binding mechanism of the triphilic polymer as compared to the amphiphilic one. In case of F-GP binding not only polar and hydrophobic forces have to be balanced, but also the tendency of the perfluoroalkyl chains to segregate, has to be taken into account. This additional driving force leads to a higher number of possible intermediates in the different steps of the interaction, as micellization/demicellization, adsorption, insertion and possibly translocation. The tendency of the inserted fluorinated chains to segregate within the membrane might play a role in the formation of membrane pores or defects.

Localization of the polymer. The second question we wanted to answer is whether the copolymer itself can permeate through the membrane. Therefore, we labelled both copolymers with tetramethylrhodamine (TMR), which was covalently attached to the GMA side groups. In order not to significantly change the block copolymer properties statistically only one label was attached per polymer chain. To label the lipid membrane BODIPY was added during GUV preparation. Excitation and emission wavelengths of these dyes were sufficiently separated to avoid crosstalk. This allowed us to simultaneously visualize the POPC membrane and the distribution of the copolymers. The experiments were performed analogously to the dye-influx experiments, *i.e.* the BODIPY stained POPC GUVs were added to a solution of TMR labelled copolymer. The appearance of TMR fluorescence within the GUVs would indicate a translocation of the copolymer through the lipid bilayer. The results are presented in Fig. 10 and 11.

The first column of Fig. 10 represents images of GP–GUV mixtures recorded about 5 min after mixing. Fig. 10a and b show an overlay of the TMR and BODIPY channels in different magnifications; Fig. 10c and d show the TMR and the BODIPY channel, respectively. Already in the TMR channel and the overview (Fig. 10a) it can be seen that there is no TMR fluorescence intensity in the interior volume of the GUVs. In the overlay of TMR and BODIPY channel (Fig. 10b) it can clearly be seen that the POPC membrane (green fluorescence) constitutes a diffusion barrier for the GP copolymer (red fluorescence). Fig. 11C shows the intensity values of the TMR and the BODIPY channel along a cut through the GUV image presented in Fig. 10b and 11A. The peaks in the green channel indicate the position of the membrane. The intensity of the red channel drops nearly to zero in between the two peaks, *i.e.* in the interior of the GUV. That indicates that GP does not translocate through the membrane. Furthermore, it is concluded that there is no surface excess of GP at the site of the membrane. These findings corroborate the results of a study of similar amphiphilic

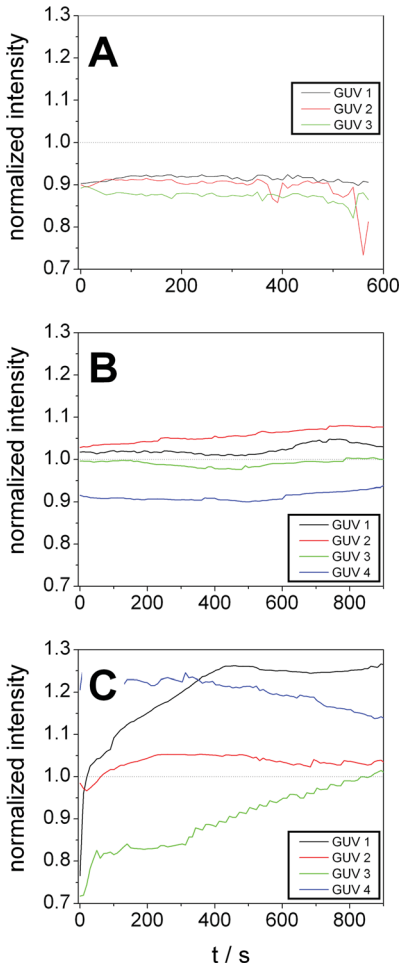

Fig. 9 Fluorescence intensities within selected POPC GUVs after addition to a dye solution containing (A) no additive, (B) GP (8 mmol L^{-1}) and (C) F-GP (7.1 mmol L^{-1}) normalized to the average fluorescence intensity of the complete image. The numbering of the GUVs corresponds to the numbering in Fig. 8.

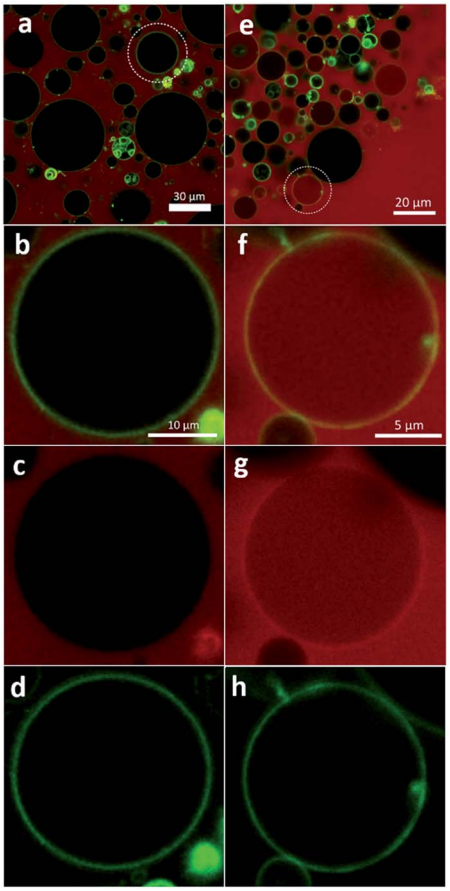

Fig. 10 Confocal laser scanning microscopy images of POPC GUVs labelled with BODIPY (green) after addition of TMR labelled GP (0.9 mmol L^{-1}) (left column) and F-GP (0.8 mmol L^{-1}) (right column). (a and e) Superposition of TMR and BODIPY fluorescence; the encircled vesicles are shown in (b and f) in a higher magnification. (c and g) TMR and (d and h) BODIPY channel of the vesicle shown in (b) and (f), respectively.

triblock copolymers with DLPC GUVs,[53] where polymer adsorption to the vesicle surface could only be observed at much higher polymer concentration and no polymer was found in the aqueous interior of the GUVs.

Very different results are obtained when the same experiment is repeated with the block copolymer F-GP (right column in Fig. 10). In Fig. 10e–g TMR fluorescence can be observed within the inner volume of the selected GUV. This indicates that the complete copolymer F-GP with its hydrophilic, hydrophobic and fluorophilic moieties is able to translocate through the lipid bilayer. Fig. 10e represents an overview of a small volume containing several GUVs. It shows that 5 min after mixing the distribution of the TMR fluorescence in the GUV suspension is inhomogeneous. Many of the GUVs are filled with F-GP, whereas numerous others show no TMR fluorescence within their lumen. This is similar to what was observed for the dye-influx experiments, discussed above and points towards a *heterogeneous graded permeabilization*.[52] In the BODIPY channel (Fig. 10h) we see an almost equal distribution of membrane staining dye, indicating that the GUV stays intact and does not disintegrate upon pore formation and copolymer translocation. Fig. 10f also shows that the highest TMR fluorescence intensity is co-localized with the fluorescence of the membrane staining BODIPY, *i.e.* the site of the membrane.

This becomes even clearer in Fig. 11D, where the intensity values along a line through the image presented in Fig. 10f and 11C are plotted. In between the peaks of the green channel the red fluorescence decreases only slightly with respect to the intensity before the first and after the second peak. Moreover, the intensity of the red channel is maximal at the position of the membrane, *i.e.* at the position of the highest BODIPY florescence. This indicates that (i) F-GP translocates through the vesicle membrane and (ii) the highest concentration of F-GP is found at the GUV membrane, *i.e.* strong adsorption and/or insertion of F-GP leads to an enrichment of the fluorinated copolymer at the membrane. This is clearly different to what was observed for GP and reveals a clear effect of the perfluoroalkyl end groups, which apparently increases the interaction with the lipid membrane.

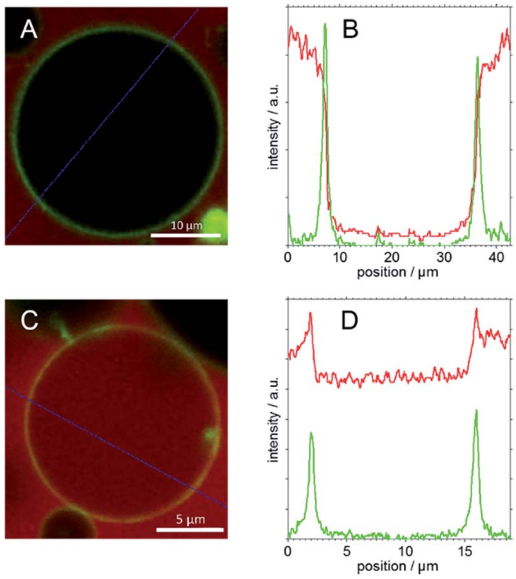

Fig. 11 CLSM images of BODIPY labelled GUVs in (A) TMR labelled GP solution and (C) TMR labelled F-GP solution and relative intensity values of red (TMR) and green (BODIPY) channels (B and D) along the blue lines drawn in (A and C), respectively.

The exact mechanism of F-GP translocation cannot be derived from the data presented here. The question remains, whether the polymer is freely diffusing through pre-formed pores or defects or whether it translocates by a sequence of adsorption, percolation[8] and desorption at the other side of the bilayer. As both, translocation and pore formation occur concomitantly the former pathway seems to be probable. Moreover, it is unlikely that the hydrophilic PGMA blocks of the copolymers may pass the hydrophobic barrier of the membrane without using any defects.

The fluorescence experiments indicate clear differences in the action of F-GP and GP and thus reveal the effect of the copolymer perfluoro end groups. The addition of perfluoro moieties leads to a stronger adsorption to POPC membranes and to the formation of membrane defects that allow the diffusion of water soluble probes as well as the translocation of the complete triphilic block copolymer. Moreover, the finding of an enhanced binding of F-GP corroborates the conclusion we have drawn from the DSC experiments.

Conclusion

The interaction of new symmetric amphi- and triphilic block copolymers with lipid membranes has been investigated. The amphiphilic block copolymers consist of a hydrophobic PPO middle block to which hydrophilic PGMA blocks are attached on either side. The triphilic block copolymer is derived from the former one by terminally attaching perfluoroalkyl chains to the PGMA blocks. These perfluoro segments are both hydrophobic and lipophobic and thus have a tendency to phase segregate in water as well as in a hydrocarbon matrix. DSC was used to study the phase transition temperature T_m of lipid membranes upon interaction with the polymers. T_m is a thermodynamic parameter that reflects the stability of the gel- and liquid crystalline phases of the membrane and therefore allows conclusions about the nature of the interactions. An extensive set of DSC data was acquired under systematic variation of the polymer concentration, the chain length of the phospholipids, the nature of their headgroups, and the addition of perfluoro moieties to the copolymer. The resulting variations in T_m are small but rather systematic. The following observations were made:

i. Decrease and increase in T_m are possible upon polymer binding, depending on the chosen conditions. The actual value of T_m is a result of a delicate balance of counteracting effects.

ii. The shift in T_m (ΔT_m) after polymer binding increases with the hydrophobic thickness of the bilayer. It is negative for the thinner DMPC and positive for the thicker DAPC membranes.

iii. ΔT_m is higher for PE headgroups than for PC headgroups, *i.e.* it increases with the capacity of the lipid headgroups to donate hydrogen bonds.

iv. ΔT_m is maximal at intermediate copolymer concentrations (1 to 2 mol%).

v. All effects are amplified by the addition of perfluoro end groups to the copolymer.

vi. Perfluoro moieties induce the tendency for phase separation within the membrane.

These findings lead to the conclusion that the binding mechanism of the polymers consists of an adsorption of the hydrophilic PGMA blocks to the headgroup layer and a concomitant insertion of the PPO blocks and perfluorinated chains into the hydrophobic part of the lipid bilayer. Clear evidence for both processes is given by the chain length and headgroup dependency of T_m. A contribution of H-bonding to the headgroup interactions is probable, as the interactions increase with the availability and accessibility of H-donors and -acceptors. It is worth noting that a positive ΔT_m was rarely reported for poloxamer binding to lipid membranes, which usually leads to a decrease in T_m.[7,9,21,22] Therefore, we think that the positive shift of T_m that we observe systematically upon binding of the PGMA containing block copolymers is due to the higher propensity of the GMA side groups to donate and to accept H-bonds. The addition of perfluoro segments to the copolymer leads to a stronger binding, the perfluoroalkyl chains acting as lipid anchors. Additionally, they induce a tendency for segregation within the bilayer.

Magic angle spinning NMR spectroscopy was applied to directly prove the insertion of the PPO blocks into the hydrocarbon membrane layer. On a sub-molecular level we could show the close proximity between PPO methyl groups and the lipid acyl chains of DMPC. This intimate contact could be shown for both fluorinated and non-fluorinated copolymer and provides unambiguous evidence for the copolymer insertion.

On a larger length scale we investigated the influence of polymer adsorption and insertion on the integrity of the membrane. By fluorescence microscopy on giant unilamellar POPE vesicles (GUVs) we could show that binding of the copolymer with perfluoro moieties leads to the formation of membrane defects that allow the influx of water soluble dyes as

well as the translocation of the complete triphilic block copolymer through the bilayer. In contrast, the binding of the non-fluorinated triblock copolymer does not or only marginally disturb the barrier function of the membrane. Only very moderate dye influx and only rare events of polymer translocation could be observed. Moreover co-localization experiments with labelled polymer and stained GUVs showed an enrichment of F-GP at the lipid membrane, indicating a strong adsorption, which could not be observed for GP.

All experiments lead to a consistent picture of the interaction of the copolymers with lipid membranes and reveal the role perfluoro segments. In comparison to the extensively studied (yet not completely understood) poloxamers the introduction of the GMA side chains and the perfluoro anchors lead to new modes of interaction and new structuring elements. The further study of these amphi- or triphilic molecules is promising, as the fine tuning of hydrogen bonding interactions, hydrophobic interactions and the segregation tendency of fluorinated moieties may lead to the controlled design of target structures, such as defined pores or channels.

Acknowledgements

The authors thank Dr Zheng Li for the synthesis of the polymers, D. Glatte for help with the CLSM measurements, and the Deutsche Forschungsgemeinschaft (DFG) for financial support (FOR 1145).

References

1 J. Y. Wang, J. M. Chin, J. D. Marks and K. Y. C. Lee, *Langmuir*, 2010, **26**, 12953–12961.
2 V. Y. Erukova, O. O. Krylova, Y. N. Antonenko and N. S. Melik-Nubarov, *Biochim. Biophys. Acta*, 2000, **1468**, 73–86.
3 S. A. Maskarinec, G. H. Wu and K. Y. C. Lee, in *Cell Injury: Mechanisms, Responses, and Repair*, ed. R. C. Lee, F. Despa and K. J. Hamann, 2005, vol. 1066, pp. 310–320.
4 R. C. Lee, L. P. River, F. S. Pan, L. Ji and R. L. Wollmann, *Proc. Natl. Acad. Sci. U. S. A.*, 1992, **89**, 4524–4528.
5 F. A. Merchant, W. H. Holmes, M. Capelli-Schellpfeffer, R. C. Lee and M. Toner, *J. Surg. Res.*, 1998, **74**, 131–140.
6 C. Y. Cheng, J. Y. Wang, R. Kausik, K. Y. C. Lee and S. Han, *Biomacromolecules*, 2012, **13**, 2624–2633.
7 M. A. Firestone, A. C. Wolf and S. Seifert, *Biomacromolecules*, 2003, **4**, 1539–1549.
8 S. Hezaveh, S. Samanta, A. De Nicola, G. Milano and D. Roccatano, *J. Phys. Chem. B*, 2012, **116**, 14333–14345.
9 G. Pembouong, N. Morellet, T. Kral, M. Hof, D. Scherman, M. F. Bureau and N. Mignet, *J. Controlled Release*, 2011, **151**, 57–64.
10 E. Amado, A. Blume and J. Kressler, *React. Funct. Polym.*, 2009, **69**, 450–456.
11 E. Amado, C. Augsten, K. Mäder, A. Blume and J. Kressler, *Macromolecules*, 2006, **39**, 9486–9496.
12 T. Demina, I. Grozdova, O. Krylova, A. Zhirnov, V. Istratov, H. Frey, H. Kautz and N. Melik-Nubarov, *Biochemistry*, 2005, **44**, 4042–4054.
13 E. Amado, A. Blume and J. Kressler, *Langmuir*, 2010, **26**, 5507–5519.
14 E. Amado, A. Kerth, A. Blume and J. Kressler, *Langmuir*, 2008, **24**, 10041–10053.
15 S. O. Kyerematen, E. Amado, A. Blume and J. Kressler, *Macromol. Rapid Commun.*, 2008, **29**, 1140–1146.
16 M. P. Krafft and J. G. Riess, *Biochimie*, 1998, **80**, 489–514.
17 E. Amado and J. Kressler, *Soft Matter*, 2011, **7**, 7144–7149.
18 S. O. Kyerematen, K. Busse, J. Kohlbrecher and J. Kressler, *Macromolecules*, 2011, **44**, 583–593.
19 S. O. Kyerematen, T. Henze, K. Busse and J. Kressler, *Macromolecules*, 2010, **43**, 2502–2511.
20 E. Feitosa and F. M. Winnik, *Langmuir*, 2010, **26**, 17852–17857.
21 J. D. Castile, K. M. G. Taylor and G. Buckton, *Int. J. Pharm.*, 2001, **221**, 197–209.
22 Y. Y. Chieng and S. B. Chen, *J. Phys. Chem. B*, 2009, **113**, 14934–14942.
23 W. M. Yau, W. C. Wimley, K. Gawrisch and S. H. White, *Biochemistry*, 1998, **37**, 14713–14718.
24 L. L. Holte and K. Gawrisch, *Biochemistry*, 1997, **36**, 4669–4674.
25 D. Huster, K. Arnold and K. Gawrisch, *J. Phys. Chem. B*, 1999, **103**, 243–251.
26 J. Jeener, B. H. Meier, P. Bachmann and R. R. Ernst, *J. Chem. Phys.*, 1979, **71**, 4546–4553.
27 G. Cevc, A. Watts and D. Marsh, *FEBS Lett.*, 1980, **120**, 267–270.
28 A. Watts, K. Harlos, W. Maschke and D. Marsh, *Biochim. Biophys. Acta*, 1978, **510**, 63–74.
29 D. Papahadjopoulos, M. Moscarello, E. H. Eylar and T. Isac, *Biochim. Biophys. Acta*, 1975, **401**, 317–335.
30 C. Schwieger and A. Blume, *Eur. Biophys. J.*, 2007, **36**, 437–450.
31 V. P. Ivanova, I. M. Makarov, T. E. Schaffer and T. Heimburg, *Biophys. J.*, 2003, **84**, 2427–2439.
32 C. h. Huang and S. Li, *Biochim. Biophys. Acta*, 1999, **1422**, 273–307.
33 E. Amado, A. Kerth, A. Blume and J. Kressler, *Soft Matter*, 2009, **5**, 669–675.
34 J. F. Nagle and S. Tristram-Nagle, *Biochim. Biophys. Acta*, 2000, **1469**, 159–195.
35 N. Kučerka, Y. Liu, N. Chu, H. I. Petrache, S. Tristram-Nagle and J. F. Nagle, *Biophys. J.*, 2005, **88**, 2626–2637.
36 M. Garavaglia, S. Dopinto, M. Ritter, J. Furst, S. Saino, F. Guizzardi, M. Jakab, C. Bazzini, V. Vezzoli, S. Dossena, S. Rodighiero, C. Sironi, G. Botta, G. Meyer, R. M. Henderson and M. Paulmichl, *Cell. Physiol. Biochem.*, 2004, **14**, 231–240.
37 M. Caffrey and J. Hogan, *Chem. Phys. Lipids*, 1992, **61**, 1–109.
38 R. Lewis, N. Mak and R. N. McElhaney, *Biochemistry*, 1987, **26**, 6118–6126.
39 C. Schwieger and A. Blume, *Biomacromolecules*, 2009, **10**, 2152–2161.
40 M. Dyck, P. Krüger and M. Losche, *Phys. Chem. Chem. Phys.*, 2005, **7**, 150–156.
41 A. Blume, *Biochemistry*, 1980, **19**, 4908–4913.
42 P. b. Hitchcoc, R. Mason, K. M. Thomas and G. G. Shipley, *Proc. Natl. Acad. Sci. U. S. A.*, 1974, **71**, 3036–3040.

43 R. Koynova and M. Caffrey, *Chem. Phys. Lipids*, 1994, **69**, 1–34.
44 M. Save, J. V. M. Weaver, S. P. Armes and P. McKenna, *Macromolecules*, 2002, **35**, 1152–1159.
45 K. Mortensen, *J. Phys.: Condens. Matter*, 1996, **8**, A103–A124.
46 Y.-l. Su, J. Wang and H.-z. Liu, *Macromolecules*, 2002, **35**, 6426–6431.
47 J. Forbes, C. Husted and E. Oldfield, *J. Am. Chem. Soc.*, 1988, **110**, 1059–1065.
48 D. Neuhaus, in *Encyclopedia of Magnetic Resonance, Vol. 5*, ed. D. M. Grant and R. K. Harris, J. Wiley & Sons, Chichester, 1996, p. 3290.
49 K. Schmidt-Rohr and H. W. Spiess, *Multidimensional Solid-State NMR and Polymers*, Academic Press Ltd, London, 1994.
50 K. L. Koster, M. S. Webb, G. Bryant and D. V. Lynch, *Biochim. Biophys. Acta*, 1994, **1193**, 143–150.
51 B. Apellániz, J. L. Nieva, P. Schwille and A. J. García-Sáez, *Biophys. J.*, 2010, **99**, 3619–3628.
52 H. Patel, C. Tscheka and H. Heerklotz, *Soft Matter*, 2009, **5**, 2849–2851.
53 R. Schöps, E. Amado, S. S. Müller, H. Frey and J. Kressler, *Faraday Discuss.*, 2013, **166**, 303–315.